Novel workflow for image-guided gamut mapping

Asaf Golan
Hagit Hel-Or
University of Haifa
Department of Computer Science
Haifa 31905, Israel
E-mail: hagit@cs.haifa.ac.il

Abstract. *We introduce a novel workflow that will hopefully open new directions of processing and improvement in image reproduction. Existing gamut mapping algorithms can be classified into two basic categories: image-independent algorithms and image-dependent algorithms. The latter algorithms produce better reproduction; however, because they are time consuming and mathematically complex, the image-independent approach is commonly used in most imaging workflows. We suggest a new workflow that attempts to approach the image-dependent mapping method without incurring significant computational drawbacks nor requiring changes in the imaging industrial standards. The proposed method attempts to choose an appropriate gamut mapping per image without reconstructing the image gamut itself and without constructing an image-specific mapping on the fly, as required by image-dependent gamut mapping methods. Specifically, image characteristics are exploited for selection of a source gamut and a gamut mapping most appropriate for a given input image from a set of available mappings. Accordingly the proposed method is named image-guided gamut mapping. We show the practicability and advantages of the suggested workflow in several specific cases. We show that better image quality is achieved for 87% of the tested images when using the suggested workflow.* © 2008 SPIE and IS&T. [DOI: 10.1117/1.2955996]

1 Introduction

Color gamut is a range of colors achievable on a given color reproduction medium. Gamut mapping, which plays an essential role in color management, aims to transform data represented under one device gamut into data represented under a different device gamut with the goal of ensuring good correspondence of overall color appearance between the original and the reproduction.

Most industrial implementations of gamut mappings are based solely on input and output device gamuts, i.e., mapping is image independent.[1–6] In typical workflows, the capturing device (camera, scanner) has a much larger gamut than the viewing device (printer, monitor), which results in a mapping that performs contraction of the larger gamut into the smaller one. This results in original image colors being compressed into, and typically not exploiting, the full destination gamut. Thus, image-dependent gamut mapping, which is dependent on the image gamut (the range of colors appearing in the image) and on the destination gamut, greatly improves image reproduction quality.[2,7–10] However, industrial designers have rejected this approach due to the intense computations and extreme overhead in terms of run time compared to the image-independent approach.

In the never-ending quest for improving image quality, the industrial focus in recent years was on the improvement of the image-independent mapping algorithms. This produced color quality changes in small increments over the years.[2–6,11] In this paper, we propose an intermediate path that attempts to approach the image-dependent mapping method without incurring significant computational drawbacks nor requiring changes in the imaging industrial standards. The proposed method attempts to choose an appropriate gamut mapping per image without reconstructing the image gamut itself and without constructing an image-specific mapping on the fly, as required by image-dependent gamut mapping methods. Specifically, image characteristics are exploited for selection of a source gamut and a gamut mapping most appropriate for a given input image. Accordingly, the proposed method is named image-guided gamut mapping.

Current workflow in the imaging industry dictates that transfer of visual information between imaging devices is performed through an intermediary representation space called the profile connection space (PCS),[12] which is a device-independent color space based on perceived color sensations, such as the CIEXYZ and the CIELAB.[12–14] Every imaging device is associated with a unique transformation between the PCS and the device specific color representation (e.g., RGB for digital cameras and scanners and CMYK for printers). This transformation does not assume any knowledge on the color distribution of the input image nor on the source device gamut and thus must support any input color (i.e., it must provide a transformation from every color coordinate in the PCS representation). In practice, the International Consortium of Color (ICC) standard dictates that the PCS to device transformation is a concatenation of an image-independent gamut mapping between the full PCS space to the subspace of the PCS representing the device gamut, and a color transformation from the device gamut (in PCS coordinates) to the device specific color space. This workflow has been standardized by the ICC (Ref. 12) and is based on the following two components:

1. *The ICC Profile.* A standard ICC profile is created for every imaging device, which includes the transformation to/from the PCS color representation and the device specific color space.

Paper 07095R received Jun. 12, 2007; revised manuscript received Feb. 22, 2008; accepted for publication Apr. 8, 2008; published online Jul. 17, 2008.

1017-9909/2008/17(3)/033004/11/$25.00

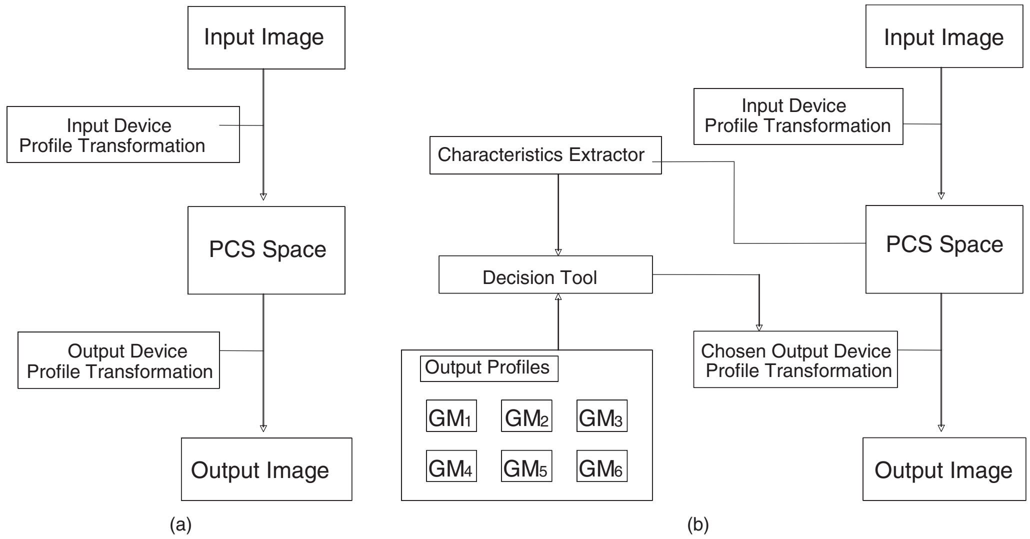

Fig. 1 Extending the CCM: (a) The ICC defined CMM. Given an input image, the CMM maps the image color values using the transformation tables or multiplication matrices stored in the device profile. (b) The proposed CMM performs image-guided gamut mapping by including a decision process that selects a gamut mapping transformation table or matrix from a set of possibilities all stored within the device ICC profile. The decision process receives as input, the characteristics of the image that is to be rendered.

2. *Color Management Module (CMM).* The CMM is an activation mechanism that actually performs the color transformations using the device ICC profile [Fig. 1(a)]. Because color transformations in the ICC profile typically supply values only for points of the color space sampled at regular grids, the CMM must implement interpolation for all color values.

The method proposed in this paper conforms to the ICC standard and can be easily incorporated into existing workflows. It extends the operation of the CMM to perform image-guided gamut mapping by including a decision process that selects a PCS-to-device transformation from a set of possibilities all stored within the device ICC profile. We note that the current ICC profile standard is defined to allow storage of a number of color transformations; thus, the suggested workflow is easily implemented without the need of redefining profiling standards.[12] Figure 1(b) shows a schematic diagram of the changes in the workflow as expressed in the CMM. The decision process receives as input, the characteristics of the image that is to be rendered. Based on these characteristics, one of the available PCS-to-device transformations is selected and implemented on the input image.

The set of PCS-to-device transformations, which differ only in the gamut mapping portion, are precomputed and stored in the device profile, independent of the input images. The set of gamut mappings differ in the type and rate of compression applied to colors in different regions of the PCS color space. The aim of the decision process is to select the compression from the set that produces the best image reproduction. In general, this correlates with maximizing the preservation of the image colors within the destination gamut.

Image-guided gamut mapping provides improved color reproduction because it selects a mapping that best approximates the optimal image-dependent mapping, in terms of minimum color loss. Additionally, because the image characteristics used are fast to compute, the improvement in reproduction quality incurs only a small overhead in terms of computation.

In support of our approach, we note that the imaging industry already allows some freedom in choice of gamut mappings in the form of rendering intents.[12] The imaging expert may set a specific type of mapping (perceptual, saturation, colorimetric), according to the workflow and gamuts of the imaging devices. For example, perceptual rendering intent will compress the full PCS space into the device gamut, whereas colorimetric intent will preserve all images colors originally within the destination gamut. The existence of rendering intents emphasizes the need to tailor gamut mappings to the visual data.

In this paper, we introduce the novel workflow and describe the image-guided gamut mapping approach, show the feasibility and advantages of using the flow, and present initial results of using the workflow on an image dataset.

2 Image Independent Versus Image Dependent Gamut Mapping

Consider the case of gamut mapping between a large source gamut and a smaller destination gamut (e.g., mapping a digital camera gamut to a printer gamut). Two common methods may be considered:

1. *Clipping.* Maps values that are in the source gamut but outside the destination gamut onto the closest colors on the boundary of the destination gamut. Source colors that are originally in the destination gamut are left untouched.

(a) (b) (c)

Fig. 2 Clipping versus compression artifacts: (a) original image, (b) gamut mapping using clipping (Note the loss of details in close up) and (c) gamut mapping using compression. (Not the loss of vividness in the close up).

2. *Compression.* Maps all colors in source gamut onto all colors in the destination gamut using a monotonic mapping. Source colors that are originally in the destination gamut will not map onto themselves.

Each method is associated with common side effects. Using clipping, different colors in the source image that are outside the destination gamut may be mapped onto the same destination color. This implies that small color variations in the mapped image may be lost. For example, the details in the yellow breast feathers and in the red head feathers in Fig. 2(a) are lost following clipping as can be seen in Fig. 2(b). Using compression, all colors in the source gamut are mapped to different colors in the destination gamut. This implies that image colors that are originally inside the destination gamut (as well as those outside the destination gamut) will not be preserved. For example, the saturated colors of Fig. 2(a) are not preserved in Fig. 2(c) following compression.

It is obvious that the most appropriate method depends on the input image. For example, input images whose colors are already within the destination gamut should be mapped mainly using clipping, whereas images with out of gamut details should be mapped using some level of compression. To bypass image dependencies and improve image quality, gamut mapping algorithms in practice typically combine clipping, nonlinear and linear compression in different regions of the color space.

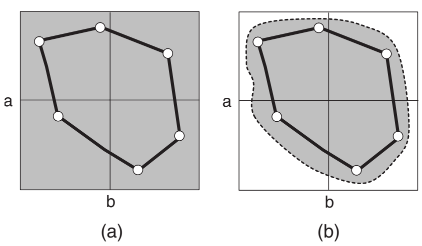

Fig. 3 Defining an effective source gamut: (a) The full perceptual color space (CIELAB, defined by the square boundary in the a-b projection of the space) is mapped to the desination gamut (defined by the enclosed polygon), (b) *A priori* knowledge of the colors that will never be used allows the mapping to consider only a subset of the perceptual color space (dashed line) in the gamut mapping. This produces, in turn, fewer color errors and a better reproduction of the color image on the output device.

(a) (b) (c)

Fig. 4 An example of using two different gamut mappings on two different images. (a) The original images. (b) Both images mapped using a gamut mapping with a narrow effective gamut in both lightness and chroma dimensions. As a result, image details are lost in the bright areas of the right image (the monitor and the dog's head in the image). (c) Both images mapped using a gamut mapping with a wide effective gamut that compresses lightness and chroma values. It can be seen that the saturated image on the left is displeasingly desaturated.

Taking into consideration the choice of mapping methods as described above, an image-dependent approach can improve reproduction quality by defining the effective boundaries of the source gamut. Consider a large source gamut (e.g., the full PCS space) and a smaller destination gamut. Gamut mapping of the full source gamut, whether using clipping or compression, will affect many colors in the source gamut. However, if it happens that the input image colors are contained within a subset of the source gamut, then a more efficient gamut mapping could be defined that better preserves the image colors. This can be done by defining an effective source gamut, which is a subset of the full source gamut and equal or close to the image gamut (see Fig. 3). Mapping is then defined from this subset alone. Compression artifacts are reduced as the effective source gamut approaches the destination gamut.

An example is shown in Fig. 4 in which two different effective source gamuts are used to define two different gamut mappings. The two gamut mappings are applied to two images that differ in their image gamut. One effective source gamut is narrow in both the chroma and the lightness dimensions. This effective source gamut is inappropriate for images with detailed highlights and shadows as these values are clipped. The second effective source gamut is wide in the chroma dimension and lightness dimension implying a mapping that compresses in both directions, making it inappropriate for images with color details. The images in Fig. 4 indicate that each of the effective source gamuts is better suited for one of the images. The image on the right is strongly affected in the lightness values, producing artifacts (loss of details) in the dark and bright areas when using the first of the two mappings (middle row). The image on the left is highly saturated and does not contain detailed bright and dark areas. The second of the two mapping produces an unpleasing desaturation effect on the image (bottom row). Thus, there is an advantage in applying image-guided gamut mapping using different gamut mappings for different images. Using any one of the two mappings would result in an inadequate mapping of one of the two images.

The advantage of image-dependent gamut mapping is in the production of better image quality obtained by setting the effective gamut to equal the image gamut. If the effective gamut is smaller than the destination gamut, then the mapping can even include image enhancement.[8]

Although, producing better quality, image-dependent gamut mapping is encumbered by the need to compute the image gamut and the gamut mapping specifically for every input image. This involves the following steps in some form or other:

1. Building the image gamut. This typically involves determining the image gamut boundary by building a gamut boundary representation.[9,15–17]
2. Determining the mapping from the image gamut to the destination gamut. This requires detection of the intersection of every mapping line with the source gamut and the destination gamut boundaries.[7–10]

Note that these two steps, which are highly time consuming, are required of any gamut mapping algorithm, whether dependent or independent. In the image-dependent approach, it must be performed for each image, whereas in the independent approach, it is performed only once in a preprocess stage and used on all images.

Additionally, an image gamut is not necessarily convex nor continuous, which requires additional gamut closure computations or causes the mapping to be very complex. Image gamut boundary, and accordingly image-dependent gamut mapping, is highly affected by isolated pixels, which have a negligible impact on the image gamut volume and on the mapping quality.

Thus, although capable of producing better image quality, most devices and color management systems assume an image-independent gamut mapping approach. In fact, the Imaging Standard assumes image independent gamut mapping and, accordingly, ICC Profiles are device-based. Current Imaging standard does not support image-dependent mappings. Incorporating image-dependent gamut mapping in the current standard requires a basic change in the standard (e.g., there will be no need for an ICC profile per device).

3 Image-Guided Gamut Mapping

In this study we introduce a compromise between the image-independent and image-dependent approaches that we termed image guided gamut mapping. Rather than calculating the gamut mapping on the fly for each image (as in the image-dependent approach), we attempt to determine an effective source gamut that best represents the image gamut for each image without incurring significant computational drawbacks. The approach bypasses the necessity of reconstructing the exact image gamut boundary and does not require the computation of the gamut mapping on the fly. Rather than computing the exact input image gamut, only a few easy-to-compute image characteristics are determined. These are used to select the best gamut mapping for the given image. Specifically, a set of effective gamuts and associated gamut mappings are designed in advance. During the rendering process, image characteristics are calculated and used to determine the gamut mapping from the set, which best suites the input image.

To achieve this goal, careful selection of image characteristics and possible mappings are necessary. A mechanism that maps the image characteristics to the appropriate mapping must be developed. In addition to efficient computation, the image characteristics should form good indicators for the mapping of choice.[12] The set of possible gamut mappings should permit a large variability in performance, allowing improvement in image rendering for a wide variety of images.

Another advantage of the image-guided gamut mapping approach is that it can be easily incorporated into the standard workflow using current imaging standards. Image-guided gamut mapping is implemented as part of a novel workflow for image rendering within the color management workflow defined by the ICC (see Section 1). The suggested workflow is easily implemented without the need of redefining profiling standards. The operation of the CMM is extended to perform image-guided gamut mapping by including a decision process that selects a gamut mapping transformation table from a set of possibilities all stored within the device ICC profile. The decision process receives as input, the characteristics of the image that is to be rendered. Figure 1(b) shows a schematic diagram of the changes in the workflow as expressed in the CMM. We note that the current ICC profile standard is defined to allow storage of a number of gamut mappings, thus the suggested workflow is easily implemented without the need of redefining profiling standards.[7] Technical details are given in Appendix A.

The image-guided gamut mapping approach differs, in principle, from previously published approaches. Earlier studies also suggested the use of image characteristics to adapt the mapping algorithm itself.[8,10] Whether this is incorporated into an image-dependent or an image-independent approach, the mapping development (step 2 in Section 2) must be performed on the fly for each image. In the image-guided workflow, image characteristics are used to choose the mapping rather than design the mapping, because these mappings are created off-line, independent of the image.

In Ref. 18, a study was presented in which image characteristics were used to determine which of a given set of five different gamut mappings best suits an image. Similar to the image-guided gamut mapping approach, their approach designs a decision mechanism based on training to perform the selection of appropriate mapping. This approach inherently differs from the image-guided approach suggested in this paper, in that the latter aims to estimate the most appropriate effective source gamut for each image in an attempt to approach the image-dependent gamut mapping scheme, whereas in Ref. 18 the goal is to determine the mapping that best suits specific classes of images (portraits, business graphics, texture-rich images, etc.) with an emphasis on the spatial informational content in the image.

Image-guided gamut mapping requires three elements: a collection of image characteristics, a set of effective gamuts and associated gamut mappings, and a mechanism for mapping image characteristics to the best gamut mapping. In the following sections, we describe the specific implementation of these elements as used in our research.

4 Image-Guided Gamut Mapping: Implementations

4.1 *Image Characteristics*

As described above, image characteristics are used to determine the best gamut and gamut mapping of a given set for each input image. These characteristics must be informative yet easily extracted at a low computational cost. The chosen image characteristics are expected to capture aspects of the image that are important to our visual sensation of image quality and thus are effective in determining the optimal gamut mapping. Accordingly, we choose to define the characteristics in the hue-lightness-chroma (HLC) color space.[14] The HLC coordinates used in the implementation of this study are the polar representation of the CIELAB coordinates.[13,14]

Because image characteristics must be efficient to compute, they are constrained to values that may be calculated with one pass over the image or over samples of the image. Image histograms can be computed efficiently, and thus, the image characteristics that were chosen are based on histograms of the HLC values of an image.

The characteristics were chosen of three types. The first set consists of basic statistical measures of the chroma and lightness coordinates. For each coordinate, the following measures were used: Mean value, standard deviation, minimum value, maximum value, 25 percentile, 50 percentile, and 75 percentile.

The second type of image characteristics are related to image content in terms of shadow and highlight regions as well as image contrast. These characteristics are known to affect perceived quality of rendered images. Three characteristics were chosen: Shadow strength (defined as the average of the lowest 4% of the lightness values in the image), highlight strength (defined as the average of the highest 5% of the lightness values in the image), and global contrast in image (defined as the normalized range of lightness values).

The third type of image characteristics measures the local spatial behavior of the image. Although these characteristics do not follow our initial assumption of histogram-based features, it has been suggested[18–20] that local spatial characteristics may relate to image artifacts that appear using incorrect gamut mapping. Allowing a single convolution of the image, this characteristic can be evaluated efficiently. Local contrast in the image is defined as the average of local differences between a pixel and its neighbors.

An additional type of image characteristic was tested that is dependent on the destination gamut used in the process: Out-of-gamut pixels ratio, which is defined as the percentage of image pixels that are outside the destination gamut.

4.2 *Set of Effective Gamuts and Gamut Mappings*

In the suggested approach, a set of mappings is defined. We assume the source gamut to be the full PCS space in accord with the ICC standard.[12] The destination gamut is a subset of this space (e.g., a printer gamut). The mappings differ in the subset of the PCS used as the effective source gamut. In general, the mappings can also differ in the transformation algorithm (e.g., clipping/compression, etc., see Section 2). For simplicity, we restrict our mappings to compression in the form of piecewise linear mappings from the effective source gamut to the destination gamut.

Similar to the definitions of the image characteristics, here too it is advantageous to define the gamut mapping transformation tables in the HLC color space. Defining the gamut mapping (and, accordingly, the effective source gamut) in this space will allow us to analyze the selection of gamut mappings for a given image and to predict its visual affect on the reproduction. Thus, it is assumed that all PCS data are first transformed to HLC.

There are infinitely many possibilities for building gamut mappings. For simplicity and as a systematic approach, the transformation tables are built based on the following principles:

1. The mapping maintains the hue coordinates.
2. Lightness is mapped first. Lightness is mapped linearly.
3. Chroma is mapped last. Chroma is mapped linearly.

The different gamut mappings in our collection vary in the manner in which lightness and chorma are mapped. Given the first principle, that the hue coordinate is maintained in the mapping, we define the gamut mapping within each hue-constant plane in the HLC space. Consider the chroma-lightness plane for a specific hue shown in Fig. 5(a). The full HLC space is shown for this hue with lightness in the range 0–100 and chroma in the range 0–181. The destination gamut boundary (which is constant over all gamut mappings in the designed set) is marked by the dark line. We denote the minimal and maximal lightness values of the destination gamut as $L\min_D$ and $L\max_D$ [see Fig. 5(a)]. The maximal values of the the chroma coordinates in each-hue plane of the destination gamut are dependent on the lightness value. Within the hue plane, for every lightness value L, the maximal chroma value in the destination gamut is denoted $C\max_D^h(L)$.

For each gamut mapping, an effective source gamut is defined. For simplicity, the effective gamut is assumed to be a convex polygon determined by the minimal and maximal lightness values denoted $L\min_S$ and $L\max_S$ [see Fig. 5(a)] and determined by the maximal chroma value within each hue plane. For simplicity, we assume that the maximal

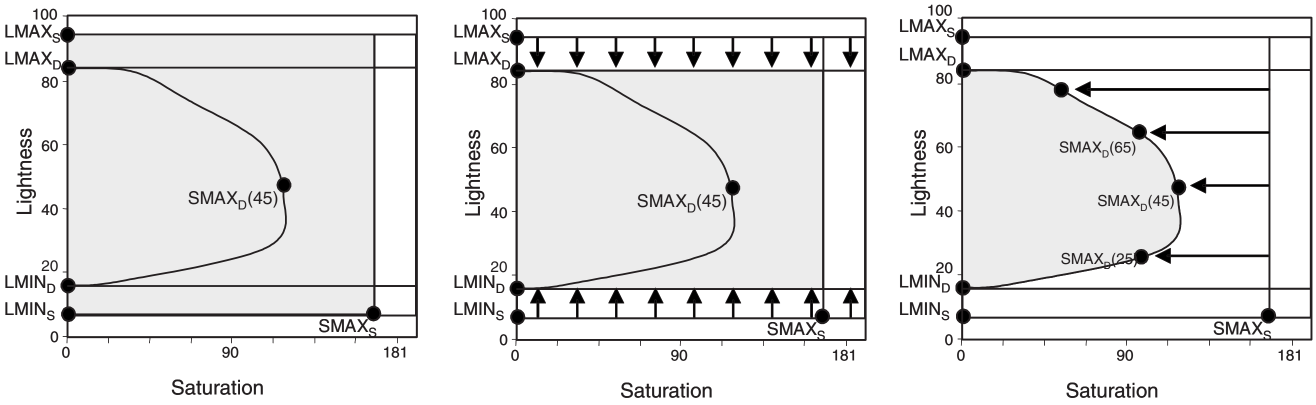

(a) (b) (c)

Fig. 5 Building a gamut mapping with an effective source gamut: (a) A slice of the HLC color space in a plane of constant hue. The corresponding slice of the destination gamut is shown as a dark line. An effective source gamut is defined in this plane by defining the minimum and maximum lightness values and the maximum chroma value: $L\,\min_S$, $L\,\max_S$, and $C\,\max_S$. The various gamut mappings defined in this study vary in these three parameters. (b) Lightness is mapped first. Lightness is mapped linearly between the range of lightness values of the effective source gamut defined by $L\,\min_S$ and $L\,\max_S$ to the range of lightness values of the destination gamut defined by $L\,\min_D$ and $L\,\max_D$. (c) Chroma is mapped last. Chroma is mapped linearly from the effective source gamut range $0-L\,\max_S$ to the destination gamut chroma range $0-L\,\max_D(L)$, which is dependent on the lightness value. Chroma values are mapped independently for each lightness value.

chroma value is constant for all lightness coordinates in all hue planes and is denoted $C\max_S$ [see Fig. 5(a)].

Following the three principles, the gamut mapping first linearly maps the lightness values of the effective source gamut to the range of lightness values of the destination gamut [Fig. 5(b)]. The chroma coordinates are then similarly mapped. For every lightness value L, the gamut mapping linearly maps the chroma coordinates between 0 and $C\max_S$ and 0 and $C\max_D^h(L)$ (Fig. 5(c)). Values outside the effective source gamut are clipped to its boundary.

Because the destination gamut is assumed constant, every gamut mapping is determined only by the parameters defining the effective source gamut: the maximal and minimal lightness values and the maximal chroma value (i.e., every gamut mapping is uniquely defined by $L\min_S$, $L\max_S$, and $C\max_S$).

It is important to understand the effect of these gamut mappings on an image. Note that the lower the value of $C\max_S$, the *less* compression of colors is performed. Note also that when the difference between $L\max_S$ and $L\max_D$ ($L\min_S$ and $L\min_D$) decreases, the compression factor in the luminance axis decreases as well.

4.3 *Image Characteristic based Gamut Mapping Selection*

Image-guided gamut mapping requires a decision tool, which is embedded in the CMM. Given a set of image characteristic values, the CMM must determine the appropriate gamut mapping to use from the collection stored in the ICC profile [see Fig. 1(b)]. To build this decision tool, a supervised classification learning approach is used in which a set of training examples serves to produce a decision rule by which new test examples can be classified. In our experiments, we use the the support vector machine (SVM),[21–23] which is a maximum margin classifier that finds a hyperplane within the high-dimensional input feature space that best separates the classes of data.

A set of training examples, which include numerous images and their best gamut mappings (determined by the visual quality of the reproduced image, see Section 5.1), were collected. For each image, a vector of image characteristic values was determined and used as input to the SVM. A leave-one-out training approach was used to determine a nonlinear decision rule dependent on the image characteristic values. Details of the training data and resulting classification is given in Section 5.

To evaluate the contribution of each image characteristic to the classification task, a feature selection process was applied. Nearest-neighbor-based feature selection[24] provides a ranking of the features in terms of their importance to the classification task. Feature selection involves the definition of an evaluation function that estimates the quality of performance for a given subset of features. A search algorithm is used to search for the subset with the highest score. The ranking of image characteristics provides numerous insights on the criteria for choosing the appropriate gamut mapping. This is discussed in Section 5.2.

4.4 *Experimental Workflow*

As a general goal to show feasibility of the image-guided gamut mapping approach, we chose the task of printing an RGB image acquired by a digital camera on an RGB printer. The images are associated with an SRGB profile (i.e., the RGB to PCS transformation is according to the SRGB standard).[25,26] The assumption of an RGB printer rather than a CMYK printer allows us to work with 3-D color spaces throughout our workflow.

The workflow transforming the input RGB data to the printer RGB requires the following steps:

$$\mathrm{RGB_{camera}} \xrightarrow{1} \mathrm{LAB} \rightarrow \overbrace{\mathrm{HLC} \xrightarrow{\text{selected GM}} \mathrm{HLC_{printerGamut}}}^{2} \rightarrow \mathrm{LAB} \xrightarrow{3} \mathrm{RGB_{printer}} \quad (1)$$

In practice, to view the images in the experiments as well as create figures for this paper, we followed the flow by a conversion to $\mathrm{RGB_{monitor}}$.

1. Transform from RGB color space to CIELAB color space using the standard transformation as defined in the SRGB color space standard[25,26] and in Ref. 14
2. Apply a gamut mapping selected from the available set. In practice, this step is performed by first mapping CIELAB to HLC and then using one of the mappings of the set described in Section 4.2 and finally mapping from HLC representation within the printer gamut back to CIELAB representation.
3. Transform from CIELAB coordinates to the $\mathrm{RGB_{printer}}$ representation using a transformation determined from printer measurements.[12,27]

The printer gamut boundary was determined using the polar sorting method as described in Ref. 16. Transformation from CIELAB to $\mathrm{RGB_{printer}}$ coordinates was determined using standard calibration testing.

5 Results

5.1 *Experiment 1: Visual Evaluation*

A set of 105 RGB images were collected varying in character. The images included indoor and outdoor scenes, under- and overexposed images, images varying in proportion and distribution of highlight and shadow regions, images with very high or very low chromaticity, etc. The collection includes several test images commonly used in the color management industry. Several examples of images in our set are shown in Fig. 6.

Using the gamut mapping algorithm described in Section 4.2, a set of 21 effective gamuts and associated gamut mappings were created. Table 1 shows the parameters $L\min_S$, $L\max_S$, and $C\max_S$ used to create the gamut and gamut mappings. Note that the effective source gamuts in cases 1–17 form significant subsets of the workflow source gamut. The 21 different mappings induce 21 different workflows [Eq. (1)].

All 105 test images were run through each of the 21 workflows obtaining 2205 rendered images. Three professional image evaluators viewed the 105 sets of images. For each set they determined which of the 21 rendered versions produced the best visible quality. The evaluators are professional image quality and color quality experts, former employees of Scitex Corp. Ltd. The images were viewed on a calibrated monitor. The images in each set were presented one at a time in 100% format, in random order. The evaluators were allowed to review and redisplay the images in each sequence as they wished, in accord with typical professional image quality evaluation.

Results of the evaluation are shown in Fig. 7. The plot shows a histogram of the number of cases for which each of the 21 workflows was chosen as producing the best visible quality. The results show that for 87% of the images, the chosen gamut mapping assumes that effective source gamut is a strong subset of the full workflow source gamut (mappings numbered 1–17). This finding implies that the original image colors do not cover the full source gamut for most of the images. Thus, mapping the full source gamut to the destination gamut without considering an appropriate effective gamut may produce unnecessary compression artifacts in most images.

The same results can also be interpreted as displaying the advantage of image-guided gamut mapping over image-independent approaches. Using an independent approach, a single effective source gamut and corresponding gamut mapping must be chosen. Considering any of the 21 mappings as the chosen image-independent gamut mapping (for example, mapping 15 in Table 1), it would be suboptimal for 86% of the images at best.

5.2 *Experiment 2: Automatic Classification of Images to Gamut Mappings*

As described in Section 3 (and Fig. 1), in the image-guided gamut mapping workflow, the CMM contains a decision tool that selects an appropriate mapping for any given image (based on image characteristics). In this paper, we demonstrate the construction of a decision tool using a classification learning approach, as described in Section 4.3. A set of training examples serves to produce a decision rule by which new test examples can be classified. The approach was implemented using two gamut mappings; however, extension to a larger set of mappings is straightforward.

The two gamut mapping algorithms chosen for the experiment (mappings 5 and 17 in Table 1) vary in the amount of compression performed in the lightness and chroma coordinates. The first of the two mappings compresses slightly in the luminance coordinate and strongly in the chroma coordinates ($L\max_S=85$, $L\min_S=0$, and $C\max_S=90$). The second mapping, compressed strongly in the lightness coordinate and slightly in the chroma coordi-

Fig. 6 Examples of the test images used in our experiments.

Table 1 Set of gamut mappings defined by the minimum and maximum values for lightness and by the maximum Chroma value of the effective source gamut (see Section 4.2).

GM Number	Min-Max Lightness $L\,\text{min}_S$–$L\,\text{max}_S$	Max Chroma $C\,\text{max}_S$
1	0–85	40
2	0–85	50
3	0–85	63
4	0–85	72
5	0–85	90
6	0–85	105
7	0–85	117
8	5–90	40
9	5–90	50
10	5–90	63
11	5–90	72
12	5–90	90
13	5–90	105
14	5–90	117
15	0–100	40
16	0–100	50
17	0–100	63
18	0–100	72
19	0–100	90
20	0–100	105
21	0–100	117

nate ($L\text{max}_S$=100, $L\text{min}_S$=0, and $C\text{max}_S$=63). All 105 test images were run through the two mappings. The ground truth was collected by the same professional image evaluators. For each of the images, the mapping that produced better reproduction quality was determined.

Each image was associated with a vector of image characteristics (Section 4.1), which was used as input to the SVM classification tool (Section 4.3). Training was performed using 85 of the 105 images. The remaining 20 images were used as test images. The classification of the 20 test images was compared to the ground truth. This procedure was repeated 100 times.

Results of the classification showed that in 83% of the cases (on average), the SVM classifier selected the same gamut mapping as the ground truth determined by the evaluators.

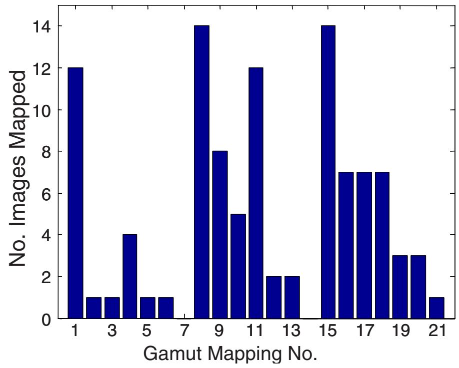

Fig. 7 Histogram displaying the number of images for which a given gamut mapping performs best. The gamut mappings are enumerated by their index given in Table 1.

5.3 *Experiment 3: Feature Selection*

To learn about the importance of each image characteristic in the classification task and in an attempt to reduce the set of image features, a feature selection process was applied using the nearest-neighbor-based feature selection[24] as described in Section 4.3. This provided a ranking of the features in terms of their importance to the classification task.

The feature selection produced the following ranking (most important to least): Highlights of luminance, medium high luminance, mean of chroma, out of gamut pixels ratio, medium high chroma, highlights and shadows contrast, mean luminance, medium chroma, shadows of luminance, standard of luminance, medium low luminance, medium of luminance, maximum chroma, medium low chroma, global contrast in image, minimum chroma, standard of chroma, minimum luminance, maximum luminance, and local contrast in the image. It was found that the produced ranking is compatible with our expected intuition. For example, “highlights of luminance” is expected to be ranked high in the list because it is largely affected by the selection of $L\text{max}_S$ and observers are typically very sensitive to artifacts in this spectral region. “Out of Gamut pixels ratio” is also expected to rank high in the list duo to high correlation with the compression factor that distinguish between the mappings. On the other hand, minimum/maximum luminance/chroma values are highly sensitive to image noise and artifacts; thus, these characteristics can be expected to rank low in the list.

Using the above ranking, an attempt was made to reduce the length of the image characteristic vector used in the classification process described in experiment 2. It was found that eliminating low-ranking image characteristics from the input vectors did not significantly deteriorate nor improve the performance (classification performance was mostly reduced by 3–7% when characteristics ranging in the last six entries in the list were removed). Eliminating characteristics in mid and high rankings significantly deteriorated the performance. It can be concluded that for the specific classification tool used in this study, the image characteristics ranked mid and high in the list are valuable for correct decision in the image-guided gamut mapping workflow.

Table 2 Ranking of image characteristics in two classification tests: Using chroma-compressing mappings (left) and luminance-compressing mappings (right).

Rank Number	Chroma-Compressing Mappings (GM 15,19)	Lightness-Compressing Mappings (GM 11,18)
1	Medium high chroma	Highlights of luminance
2	Mean of chroma	Medium-high luminance
3	Out-of-gamut pixels ratio	Medium luminance
4	Highlights of luminance	Standard of luminance
5	Medium-high luminance	Shadows of luminance
6	Highlight and shadows contrast	Mean of luminance
7	Medium luminance	Medium-low chroma
8	Medium-low chroma	Maximum chroma
9	Maximum luminance	Medium chroma
10	Medium chroma	Maximum luminance
11	Minimum chroma	Standard of chroma
12	Global contrast	mean of chroma
13	Maximum chroma	Minimum chroma
14	Standard of luminance	Global contrast in image
15	Minimum luminance	Highlights and shadows contrast
16	Standard of chroma	Minimum luminance
17	Shadows of luminance	Out-of-gamut pixels ratio
18	Medium-low luminance	Medium high chroma
19	Mean of luminance	Local contrast
20	Local contrast	Medium-low luminance

5.4 *Experiment 3: Automatic Classification of Images to Gamut Mappings II*

To further study the relationship between image characteristics and choice of gamut mapping, a second classification test was performed. In this case, using pairs of mappings that differ in the amount of compression in one of the coordinates alone. The pairs of mappings differ in the amount of chroma compression (mappings 17 and 21 in Table 1) or in the amount of lightness compression (mappings 11 and 18 in Table 1).

All 105 test images were run through the pair of mappings in each case. The ground truth was collected by the same professional image evaluators. For each of the images, the mapping that produced better reproduction quality was determined. As in the previous test, each image was associated with a vector of image characteristics (Section 4.1), which was used as input to the SVM classification tool (Section 4.3). Training was performed using 85 of the 105 images. The remaining 20 images were used as test images. The classification of the 20 test images was compared with the ground truth. This procedure was repeated 100 times.

The classification results showed 91% successful classification for the classification of chroma compressing mappings and 85% for the lightness compressing mappings. As in the previous test, feature selection was applied and a ranking of the informativeness of the image characteristics was determined. Results of the ranking are shown in Table 2.

In general, the most informative image characteristics were those associated with the coordinate that was compressed; for the chroma-compressing mappings, the chroma-based characteristics were ranked high in the list, while for the lightness-compressing mappings, the lightness-based characteristics were ranked high in the list (an exception is the characteristic ranked fourth in the chroma-compressing case). The two experiments were mostly consistent between them and consistent with the previous experiment in terms of performance and ranking of image characteristics. Although some variations in ranking occur in the low-ranked characteristics (e.g., minimum luminance and local contrast in the image), consistency exists on the whole.

Another point of interesting is the fact that, in general, the results of this experiment were better than the results of the previous experiment (Section 5.1), which implies that the decision between gamut mappings when assumptions are made on both luminance and chroma axes, is more complex as expected.

6 Discussion and Conclusion

In this study, we introduce an approach that compromises between the image-independent and image-dependent gamut mapping approaches, namely, image-guided gamut mapping. The goal is to approach image-dependent quality without the need to compute image gamut and image-specific mappings on the fly. The method attempts to approximate the image gamut by determining an appropriate effective source gamut. Specifically, a few easy-to-compute image characteristics were exploited to determine the best gamut and gamut mapping for a given image, from among a finite collection of possibilities. We showed the practicability and advantages of the suggested workflow in several specific cases. It was shown that better image quality is achieved for 87% of the tested images when using a gamut mapping that assumes a smaller input gamut. In this paper, we also showed the strong connection between the image characteristics and the chosen gamut mapping by ranking the importance of the characteristics in the classification process using a feature selection tool. We showed that the produced ranking is meaningful and in most cases expected.

We emphasize that this paper introduces a new framework for color management and does not presume to suggest an actual implementation outperforming industrially designed gamut mappings. We demonstrated feasibility of the approach using standardized mappings and assumptions. We suggest that using more advanced gamut mapping algorithms will enhance even further the distinction between the current workflow and the image-guided gamut mapping–based workflow presented in this paper.

We further note that additional image characteristics will improve the decision efficiency. Specifically, characteristics that are spatially dependent are expected to strongly influence the choice of gamut. For example, existence of continuous colorful regions, details in highlight or shadow areas, and spatial distribution of the illumination in the image are expected to produce more accurate mapping decisions. However, one must still maintain low computation cost of the characteristics. Additionally, in our tests we assumed a simplified subspace of the HLC space as the effective source gamut of the mapping (Section 4.2). This subspace was rectangular for every hue, determined by $L\max_S$, $L\min_S$, and $C\max_S$. This causes a strong compression of chroma values for HLC colors with high and low lightness values. A better representation of the effective source gamut is to more closely follow the output gamut (e.g., in a cone-like representation for the printer gamut). Additionally, we used a standard learning tool (SVM) to map image characteristics to gamut mapping. This is a simplified approach.

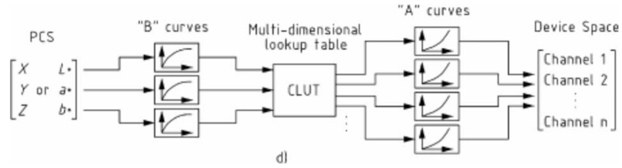

Fig. 8 The LutBtoA tag–one of the basic tags allowed by the ICC profile, supplies processing elements that are required for the standardized algorithmic flow that is shown as a flow diagram. It defines a gamut mapping from PCS to DCS. Taken from Ref. 12.

Incorporating knowledge and heuristics used by color quality experts is imperative in order to produce high quality results.

The image-guided gamut mapping approach is easily encompassed in the color management standards and forms a novel workflow that will, hopefully, open new directions of processing and improvement in image reproduction.

Appendix A: Incorporating Image-Guided Gamut Mapping in the ICC Standard

As described in Section 1, current industrial workflow has been standardized by the ICC (Ref. 12) and requires the association of an ICC profile with every imaging device. Device profiles provide color management systems with the information necessary to convert color data between the device color space (DCS) and the device-independent color space, called the profile connection space (PCS).

The standard allows several standardized algorithmic flows organized as tags. Each tag comprises a collection of processing elements, including LUT, matrix, and one-dimensional input and output curves. Mappings from the PCS to/from the DCS are coded into the tags where the type of tag and the use of the processing elements associated with the tag is chosen by the device profile designer. An example of a standard algorithmic flow is shown in Fig. 8. The ICC profile of a given device may contain several optional mappings (coded in several tags) between the color spaces. The choice of mapping to be used from the profile is typically determined by the CMM. Figure 9 shows the ICC profile structure.

The profile includes the following elements[12]

1. Profile header, which provides general information on the specific profile including profile size, version number, default CMM type, etc.
2. Profile tag table, which is the table of contents for the tags and contains a count of the number of tags in the structure and a pointer to each tag
3. Tagged element data, which comprise a collection of processing elements in each tag

The current standard supplies ICC profiles with three standard mappings from the PCS to the DCS, each mapping is associated with one of the standard rendering intents.[12] Each mapping is coded within a tag in the ICC profile. The image-guided gamut mapping approach is easily incorporated into the ICC standard by adding additional mappings from PCS to DCS using the available standard algorithmic flows (i.e., using standard tag types, such as type LutBtoA, Fig. 8). The CMM will determine which of the mappings to use for each image. Note that the transformation from PCS

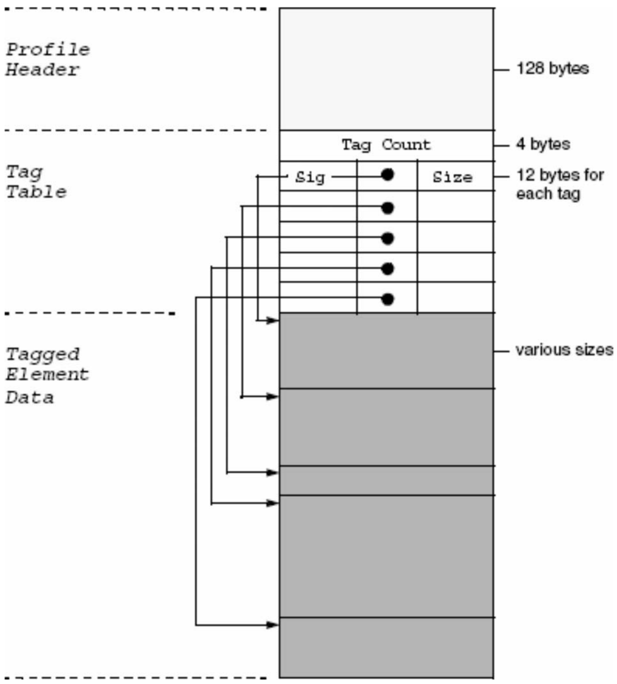

Fig. 9 The ICC profile structure. The profile includes a header, profile tag table, and the tagged element data. Taken from Ref. 12.

to DCS actually involves two stages. The first maps from the full PCS to the device gamut represented in the PCS space. The second maps from the device gamut in PCS space to the DCS. The mapping stored in the profile tags is a concatenation of these two transforms. In the image-guided gamut mapping framework, the PCS to DCS mappings all share the same second stage, namely, the mapping from device gamut in PCS space to the DCS.

References

1. J. Morovic and M. R. Luo, "The fundamentals of gamut mapping: a survey," *J. Imaging Sci. Technol.* **45**(3), 283–290 (2001).
2. G. Braun and M. Fairchild, "Gamut mapping for pictorial images," in *Proc.-TAGA* 645–660 (1999).
3. E. D. Montag and M. D. Fairchild, "Psychophysical evaluation of gamut mapping techniques using simple rendered images and artificial gamut boundaries," *IEEE Trans. Image Process.* **6**(7), 977–989 (1997).
4. R. S. Gentile, E. Walowit, and J. P. Allebach, "A comparison of techniques for color gamut mismatch compensation," *J. Imaging Technol.* **16**(5), 176–181 (1990).
5. L. Macdonald, "Gamut mapping in perceptual colour space," presented at IS&T and SID's Color Imaging Conference: Transforms and Transportability of Color, pp. 193–196 (1993).
6. J. Morovic, "To develop a universal gamut mapping algorithm," PhD thesis, University of Derby, United Kingdom (1998).
7. S. Kim, C. Lee, K. Kim, C. Lee, and Y. Ha, "Image-dependent gamut mapping using a variable anchor point," *Proc. SPIE* **3300**, 129–137 (1998).
8. H. Kotera, M. Suzuki, T. Mita, and R. Saito, "Image-dependent color mapping for pleasant image renditions," *Proc. SPIE* **4421**, 463–466 (2002).
9. R. Satio and H. Kotera, "Image-dependent three-dimensional gamut mapping using gamut boundary descriptor," *J. Electron. Imaging* **13**(3), 630–638 (2004).
10. M. Wolski, J. R. Allebach, and C. A. Bouman, "Gamut mapping: Squeezing the most out of your color system," in *Proc. IS&T SID 2nd Color Imaging Conf.: Color Science, Systems and Applications*, pp. 89–92 (1994).
11. E. D. Montag and M. D. Fairchild, "Gamut mapping evaluation of chroma clipping techniques for three destination gamuts," in *IS&T/SID 6 Color Imaging Conf.*, Scottsdale, 42, pp. 57–61 (1998).
12. I. C. Consortium, ICC Specifications, http://www.color.org/icc_specs2.html
13. G. Wyszecki and W. Stiles, *Color Science: Concepts and Methods, Quantitative Data and Formulae*, Wiley, Hoboken, NJ, (1982).
14. M. D. Fairchild, *Color Appearance Models*, Addison-Wesley, Reading, Mass. (1998).
15. R. Saito and H. Kotera, "Extraction of image gamut surface and calculation of its volume," in *Proc. IS&T and SID 8th Color Imaging Conf.*, pp. 330–333 (2000).
16. J. Morovic and M. R. Luo, "Calculating medium and image gamut boundaries for gamut mapping," *Color Res. Appl.* **25**(6), 394–401 (2000).
17. T. J. Cholewo and S. Love, "Gamut boundary determination using alpha-shapes," in *Proc. IS&T and SID 7th Color Imaging Conf.* pp. 200–203 (1999).
18. P. Sun and Z. Zheng, "Selecting appropriate gamut mapping algorithms based on a combination of image statistics," *Proc. SPIE* **5667**, 211–219 (2005).
19. P. S. J. Morovic, "Methods for investigating the influence of image characteristics on gamut mapping," in *IS&T/SID 7 Color Imaging Conf.* Scottsdale, pp. 138–143 (1999).
20. N. Bonnier, F. Schmitt, H. Brettel, and S. Berche, "Evaluation of spatial gamut mapping algorithms," in *Proc. IS&T and SID 14th Color Imaging Conf.* (2006).
21. V. N. Vapnik, *The Nature of Statistical Learning Theory*, Springer, New York (1995).
22. V. N. Vapnik, *Statistical Learning Theory*, Wiley, Hoboken, NJ (1998).
23. C. J. C. Burges, "A tutorial on support vector machines for pattern recognition," *Data Min. Knowl. Discov.* **2**(2), 121–167 (1998).
24. A. Navot, L. Shpigelman, N. Tishby, and E. Vaddia, "Nearest neighbor based feature selection for regression and its application to neural activity," in *Advances in Neural Information Processing Systems 18*, Y. Weiss, B. Schölkopf, and J. Platt, Eds., pp. 995–1002, MIT Press, Cambridge, MA (2006).
25. M. Stokes, M. Anderson, S. Chandrasekar, and R. Motta, "A standard default colour space for the internet: SRGB," http://www.w3.org/Graphics/Color/sRGB.html
26. I. E. Commission, IEC 61966-2-1:1999, http://www.color.org/sRGB.html
27. E. C. Initiative, Eci 2002 target, http://www.eci.org/eci/en/033_eci_2002_target.php

Asaf Golan received his BSc and his MSc in mathematics and computer science from Haifa University, Haifa, Israel in 1999 and in 2008, respectively. From 1999 to 2005, he also worked as an Imaging Algorithms Developer in CREO-SCITEX and in Intel (OPLUS). From 2005 he serves as a consultant for imaging companies. His main interests are color management, color vision and image processing.

Hagit Hel-Or received her PhD degree in computer science in 1994, from the Hebrew University, Jerusalem, Israel. Dr. Hel-Or was a postdoctoral fellow for two years in the Vision Group in the Department of Psychology at Stanford University. She was with the Department of Mathematics and Computer Science at Bar-Ilan University, Ramat-Gan, Israel, for two years. Currently, Dr. Hel-Or is appointed as a faculty member in the Department of Computer Science at the University of Haifa, Israel. Her research area is in the field of imaging science and technologies and includes color vision, image processing, computational and human vision.